$$\Delta H_f = E_{RHF}(C_nH_m) + E_{corr}(C_nH_m) + E_{zpt}(C_nH_m) - nH(C,\text{graphite}) - (m/2)H(H_2,\text{gas}) \quad (4)$$

expression for the ideal gas-phase heat of formation at 0 K, with eq 3 furnishes

$$E_{corr}(C_nH_m) = n\{H(C,\text{graphite}) - GE_{RHF}[C]\} + m\{\tfrac{1}{2}H(H_2,\text{gas}) - GE_{RHF}[H]\} - E_{zpt}(C_nH_m) \quad (5)$$

It has been shown that the zero-point energies (E_{zpt}) of hydrocarbons are linear functions of n and m.[26] Therefore

$$E_{corr}(C_nH_m) = nA + mB + C$$

where A, B, and C are constants: aromatic hydrocarbons whose heats of formation are adequately described by eq 3 have correlation energies that are linear functions of the numbers of carbon and hydrogen atoms. This result is consistent with the ability of SCF energy differences (even in finite basis sets) to provide accurate enthalpy changes for homodesmic reactions involving only benzenoid aromatics. It is also consistent with the inability of ab initio SCF energies to provide good heats of reaction and formation for the nonbenzenoids azulene, acenaphthylene, and biphenylene, when either homodesmic reactions or group-equivalent schemes are employed: "nonregular" effects of electron correlation are present that cannot be accounted for in either scheme. This conclusion is consistent with the observed improvement of the naphthalene → azulene isomerization energy when electron correlation to second order is included.

This work demonstrates that aromatics of even moderate size are amenable to accurate ab initio study. Future application of the ab initio methods may be to molecules with deformed benzene rings, such as the cyclophanes and paracyclophanes, or to benzenoids that are either difficult to prepare or reactive. Ab initio calculation will frequently not be the method of choice, since more economical molecular mechanics methods can be quite successful. But we note that, except for benzene itself, the semiempirical AM1 method does not furnish good heats of formation for the aromatics; positive deviations from experiment of 10 kcal/mol or more are not unusual, e.g., 13.4 kcal/mol for chrysene. The AM1 geometries, however, are generally superior to the ab initio values and are comparable to those obtained by molecular mechanics. Heats of formation for many aromatics, obtained with the AM1 predecessor MNDO, have been reported by Hites and Simonsick;[27] MNDO values show positive deviations similar to those found with AM1, e.g., 11.9 kcal/mol for chrysene.

Acknowledgment. This research was supported, in part, by Grants 666356, 667253, and 668248 of the PSC-CUNY Research Award Program of the City University of New York and a grant of computing time from the City University Committee on Research Computing. Part of this work was conducted, with vector programs developed by us (The Queens College Quantum Chemistry Package), using the Cornell National Supercomputer Facility, a resource of the Center for Theory and Simulation in Science and Engineering at Cornell University, which is funded in part by the National Science Foundation, New York State, and the IBM Corporation and members of the Corporate Research Institute.

(26) Schulman, J. M.; Disch, R. L. *Chem. Phys. Lett.* **1985**, *113*, 291.

(27) Hites, R. A.; Simonsick, W. J., Jr. *Calculated Properties of Polycyclic Aromatic Hydrocarbons*; Physical Sciences Data 29; Elsevier: Amsterdam, 1987.

Hydration Effects on S_N2 Reactions: An Integral Equation Study of Free Energy Surfaces and Corrections to Transition-State Theory

Shawn E. Huston,† Peter J. Rossky,* and Dominic A. Zichi‡

Contribution from the Department of Chemistry, University of Texas at Austin, Austin, Texas 78712. *Received December 20, 1988*

Abstract: New ab initio quantum chemical calculations and the extended RISM integral equation method are used to examine the aqueous phase S_N2 reaction of chloride with methyl chloride. Behavior in the region around the transition state is emphasized. By application, it is shown that the integral equation approach is particularly effective for examining the shape of the free energy surface, the variation of results with solvent model, and the relative contributions of energy and entropy to the net free energy. Further, it is shown that in the limiting case of fast reaction dynamics and rapid charge transfer near the transition state, the correction to the transition-state theory rate constant can be estimated within the integral equation framework; results obtained agree reasonably with those derived from extensive dynamical simulation.

I. Introduction

Bimolecular nucleophilic substitution reactions of the type $X^- + CH_3Y \leftrightharpoons CH_3X + Y^-$ are among the most widely studied chemical reactions.[1,2] Investigations of such reactions have played an important role in the development of fundamental ideas in physical organic chemistry. In particular, these charge-transfer reactions provide a dramatic example of the influence of the solvent on chemical reaction rates.[3] The gas-phase and aqueous solution reaction rate constants for such reactions typically differ by 20 orders of magnitude.[4]

Recently, theoretical efforts have begun to address the description of such reactions in solution at a fully molecular level, with emphasis on the prototype case $X = Y = Cl^-$. In particular, both the free energy surface for the adiabatic motion of reactants to products in water[1] and the solvent dynamical contributions to

† Present address: The James Franck Institute and the Department of Chemistry, The University of Chicago, Chicago, IL 60637.
‡ Present address: Department of Chemistry, University of Colorado, Boulder, CO 80309.
* Author to whom correspondence should be addressed.

(1) Chandrasekhar, J.; Smith, S. F.; Jorgensen, W. L. *J. Am. Chem. Soc.* **1985**, *107*, 154.
(2) Shaik, S. S. *J. Am. Chem. Soc.* **1984**, *106*, 1227.
(3) Olmstead, W. N.; Brauman, J. I. *J. Am. Chem. Soc.* **1977**, *99*, 4219.
(4) Tanaka, K.; Mackay, G. I.; Payzant, J. D.; Bohme, D. K. *Can. J. Chem.* **1976**, *54*, 1643.

0002-7863/89/1511-5680$01.50/0

the reaction rate[5] have been the subject of recent large-scale computer simulation studies.

In a novel application of ab initio quantum chemistry and classical simulation methods, Jorgensen and co-workers calculated the aqueous solution reaction free energy profile for the symmetrical nucleophilic displacement reaction between chloride ion and methyl chloride:[1]

$$Cl^- + CH_3Cl' \rightarrow ClCH_3 + Cl'^-$$

In this calculation, the gas-phase electronic energy surface for collinear reaction was determined, as was a potential function for interaction of water with the reactant complex as a function of reaction coordinate. The parametrized potentials were then used, with Monte Carlo simulation, to determine the equilibrium solvation free energy as a function of reaction progress between the transition state and reactants (or products). Combined with the gas-phase potential, one obtains a solution-phase analogue of the quantum mechanical electronic potential energy surface for an isolated set of reactants.

One of the important results of this calculation is that the resulting free energy of activation compares well with the experimental estimate.[1] Correspondingly, the transition-state theory rate constant k^{TST} should be determinable with reasonable accuracy employing this result.[6]

The calculation of k^{TST}, the upper bound theoretical prediction for the reaction rate, utilizes the continuous equilibrium solvation of the reacting species by the solvent and does not include the dynamical consequences of coupling of solvent fluctuations to reactant motion. As has been discussed elsewhere,[7-9] such coupling can significantly influence the frequency of ultimate success in traversing the transition state to products. As emphasized by Hynes and co-workers, the shape of the barrier to reaction at the transition state provides a measure of the reaction time scale, which can be compared with the ambient solvation relaxation time, providing an estimate of the solvent dynamical correction to the transition-state theory prediction for the rate.[8] For reactions of the type under discussion here, it is clear that the free energy picture provides a reasonable approximation to the kinetic problem, accounting for the dramatic solvation effects observed experimentally. Nevertheless the dynamic aspects remain of interest.

Extensive simulation studies of the reaction dynamics for a model reaction in aqueous solvent similar to the one above have been successfully interpreted in terms of a nonequilibrium solvation model by Hynes, Wilson, and co-workers.[5,8c] Their results indicate that the critical reactive motion occurs sufficiently fast that the solvent is effectively frozen; reaction occurs on an instantaneous (nonadiabatic) solvation barrier, necessarily higher in energy than that for equilibrium solvation, and the rate is concomitantly lower.

While a better understanding of the nature of the above solution-phase ion–molecule reaction has been afforded by the results of statistical mechanical simulations, computer simulation methods are computationally intensive and therefore remain of limited feasibility. Consequently, there is significant interest in the development and application of alternative approximate theoretical approaches to the investigation of such condensed phase phenomena.

In this paper, we focus on the use of the extended RISM integral equation method[10-14] to study the reaction free energy profile and related quantities for this prototypical S_N2 exchange reaction. Extended RISM is a generalization of the Ornstein–Zernike-like RISM equation, developed by Chandler and co-workers.[15] The extension permits rapid calculation of qualitatively reliable results for the pair correlation functions for polar and ionic molecules from knowledge of the relevant interaction potentials between atomic sites in molecular pairs.

The theory has proven to be an effective means of assessing solution structural and thermodynamic properties.[10] Most recently, the method has been used to investigate molecular conformational equilibria,[11] the potential of mean force for the hydrolysis of *t*-BuCl,[12] and interaction potential truncation effects on the structure and thermodynamics of ionic solutions.[13] A preliminary application to the system of interest here has been reported previously.[14]

In the present article, we examine the collinear reaction free energy surface in more detail and consider variations in solvent polarity. Of most importance, we emphasize the behavior of the free energy surface in the vicinity of the transition state, where the origins of the dynamical corrections lie.

To do this, our calculations include both new quantum chemical modeling and extended RISM efforts. In addition to calculating equilibrium quantities, we show that the analytic nonadiabatic solvation theory of Hynes et al.[8] can be implemented in the extended RISM context to obtain an estimate of dynamical corrections to k^{TST} in the frozen solvent limit. This result is applied to the symmetrical S_N2 exchange reaction.

We begin in section II with a discussion of the computational scheme and the modeling of the system, including our reparametrization of the transition-state region for the gas-phase reaction surface and the solute–solvent potentials. In section III, we discuss first the gas-phase potential energy surface. We then proceed with a discussion of the reaction thermodynamics (free energy, energy, and entropy) and the variation of the results with solvent polarity. Completing our description of the charge-transfer reaction, we present our formal and numerical results for the nonadiabatic solvent contributions to the reaction rate constant. Section IV contains the conclusions.

II. Computational Methods

The reaction system is modeled as a single polyatomic solute at infinite dilution with variable bond lengths and interaction potentials obtained from new ab initio calculations and from previous work on the system by Jorgensen and co-workers.[1] In this section we describe in detail both the gas-phase reaction coordinate determination and the solution-phase model parametrization.

A. Gas-Phase Reaction Pathway. The minimum energy pathway (MEP) between the transition state and products for this symmetric transfer reaction was determined by using the GAUSSIAN 82[16] ab initio molecular orbital program. Calculations were performed at the restricted Hartree–Fock level using the 6-31G* basis set. This was previously assessed as a reasonable level of the theory,[1] and its use here ensures consistency with the earlier work from Jorgensen's lab. We have performed the additional quantum chemical calculations to accurately characterize the reaction near the transition state.

The shape of the gas-phase barrier is of considerable interest in this calculation as it contributes to the curvature of the solution-phase barrier, which is not easily obtained from either computer simulation[5] or experiment.[17] Further, the reaction coordinate generated by the authors of ref 1 is the result of quantum chemical calculations performed for structures that correspond largely to the reactant/product regions of the potential energy surface. The resulting reaction coordinate is therefore suspect in the barrier region.

(5) Bergsma, J. P.; Gertner, B. J.; Wilson, K. R.; Hynes, J. T. *J. Chem. Phys.* **1987**, *86*, 1356.
(6) Hynes, J. T. In *The Theory of Chemical Reaction Dynamics*; Baer, M., Ed.; Chemical Rubber: Boca Raton, FL, 1985; Vol. IV, p 171.
(7) Ladanyi, B. M.; Hynes, J. T. *J. Am. Chem. Soc.* **1986**, *108*, 585.
(8) (a) van der Zwan, G.; Hynes, J. T. *J. Chem. Phys.* **1982**, *76*, 2994. (b) van der Zwan, G.; et al. *Ibid.* **1983**, *78*, 4174. (c) Gertner, B. J.; Bergsma, J. D.; Wilson, K. R.; Lee, S.; Hynes, J. T. *J. Chem. Phys.* **1987**, *86*, 1377.
(9) Hynes, J. T. *J. Stat. Phys.* **1986**, *42*, 149.
(10) Rossky, P. J. *Pure Appl. Chem.* **1985**, *57*, 1043.
(11) Zichi, D. A.; Rossky, P. J. *J. Chem. Phys.* **1986**, *84*, 1712.
(12) Jorgensen, W. L.; Buckner, J. K.; Huston, S. E.; Rossky, P. J. *J. Am. Chem. Soc.* **1987**, *109*, 1896.
(13) Brooks, C. L., III *J. Chem. Phys.* **1987**, *86*, 5156.
(14) Chiles, R. A.; Rossky, P. J. *J. Am. Chem. Soc.* **1984**, *106*, 6867.
(15) Chandler, D. In *The Liquid State of Matter; Fluids, Simple and Complex*; Montroll, E. W., Lebowitz, J. L., Eds.; North-Holland: Amsterdam, 1982; p 275.
(16) Hehre, W. J.; Radom, L.; Schleyer, P. v. R.; Pople, J. A. *Ab Initio Molecular Orbital Theory*; Wiley: New York, 1986.
(17) Fleming, G. R. *Chemical Applications of Ultrafast Spectroscopy*; Oxford University Press: New York, 1986.

We employ an alternative route to the calculation of the MEP for this reaction system, compared to that of Jorgensen's group. This alternative ensures correct identification of the MEP in the transition-state region. The calculated results are also used to reevaluate the solvent–solute potential functions used in this work in the transition-state region.

As mentioned above, we consider only those approaches of the nucleophile that render a collinear Cl–C–Cl′ configuration.[1,14] (For convenience, throughout we will identify Cl′ as the leaving group.) This restriction is in keeping with the notion of the S_N2 mechanism as proceeding via backside attack and considerably reduces the dimensionality of the problem, thereby facilitating calculation of the MEP. A more elaborate description is not called for in the present work.

The reaction path can be conveniently described in terms of symmetric and asymmetric stretch coordinates of the Cl–C–Cl′ triple. Denoting atomic pair bond lengths by the symbol r_{ij}, we have the convenient symmetric combination

$$r_S = r_{CCl} + r_{CCl'}$$

and the asymmetric combination

$$r_A = r_{CCl'} - r_{CCl}$$

We note that the corresponding vibrational normal coordinates are given simply in terms of r_S and r_A.[18]

As dictated by symmetry, the transition state for this reaction[1] is characterized by a value of zero asymmetric stretch of the Cl–C–Cl′ atoms, with the direction of the reaction coordinate at the transition state lying along the asymmetric stretch coordinate. The MEP in this region therefore runs along the direction of asymmetric stretch and is defined by the energetic requirements for motion in the orthogonal, nonreactive, coordinates. The reaction path can then be determined by finding the minimum energy symmetric stretch configurations for fiducial values of asymmetric stretch. Practically, this amounts to performing a parabolic fit of ab initio gas-phase energies U_0 calculated along a linear search direction that samples the quantity r_S for fixed r_A[19] and requiring for the MEP[7] that

$$(\partial U_0/\partial r_S)_{r_A} = 0$$

This procedure results in r_A as the effective one-dimensional reaction coordinate.

The numerical results of such calculations will be presented in section III.A.

B. Solution-Phase Thermodynamics. The free energy surface for the aqueous-phase reaction was calculated from the extended RISM integral equation theory for the solvation structure about the reaction species.[10] We omit a detailed account of the theory, which has been previously discussed at length,[11,20] and recapitulate only the essential elements as they pertain to the calculation of solvation free energy differences.

The integral equation approach provides the pair distribution functions between atomic sites in the solution, as the result of the solution of a set of coupled nonlinear integral equations. The input consists only of the component species molecular geometries, intermolecular potentials, and state conditions of temperature T and composition (or densities). In the present context, we treat the reactant set as a single molecular complex, with geometry determined by reaction coordinate, surrounded by an infinite amount of solvent at the normal bulk density. We denote this solvent density as ρ with no subscript, as only this one component has a variable density at these infinite dilution conditions.

For a single rigid polyatomic solute u at infinite dilution in a solvent v the extended RISM excess free energy of solvation can be expressed as[12,21]

$$A^{ex}/k_BT = 4\pi\rho\sum_{uv}\int_0^\infty dr\, r^2\{\tfrac{1}{2}h_{u,v}^2(r) - c_{u,v}(r) - \tfrac{1}{2}h_{u,v}(r)\, c_{u,v}(r)\} \quad (1)$$

where h and c are the total and direct solute–solvent site–site pair correlation functions, respectively, and the summation is over all solute–solvent site pairs. ρ is the density of the pure solvent at 1 atm of pressure and absolute temperature T, and k_B is Boltzmann's constant.

This closed form expression for the excess chemical potential directly uses the solutions of the extended RISM equation but is equivalent to the more familiar and general charging scheme[11] when used in this way.

The solute–solvent and solvent–solvent interactions are described via the 12–6–1 potential

$$U_{\alpha\gamma}(r) = \sum_i^{n_\alpha}\sum_j^{n_\gamma}\left\{\frac{A_{ij}}{r_{ij}^{12}} - \frac{C_{ij}}{r_{ij}^{6}} + \frac{q_iq_j}{r_{ij}}\right\} \quad (2)$$

where α is a solvent molecule, γ is a solute or solvent molecule, and n_γ is the number of interaction sites within a molecule of species γ. q_i is the charge associated with site i, and A_{ij} and C_{ij} are the corresponding Lennard-Jones coefficients. Here we use the TIPS prescription for the combining rules, namely $A_{ij} = (A_i^2A_j^2)^{1/2}$ and correspondingly for C_{ij}.

We will also evaluate separately the energetic and entropic contributions to the free energies, using standard temperature derivatives of this quantity via finite differences of results obtained at different temperatures.[11,22]

C. Model Potentials. For water we adopt the simple point charge (SPC) model,[23] which provides a reasonable description of pure water and is well suited to the integral equation calculation. This model has a rigid idealized geometry consisting of OH bond lengths of 1.0 Å and a tetrahedral bond angle. The interaction parameters are $A_0^2 = 6.294 \times 10^5$ kcal mol^{-1} Å^{12}, $C_0^2 = 625.5$ kcal mol^{-1} Å^6, and $q_0 = -2q_H = -0.82e$. As noted in earlier work, the introduction of a small repulsive Lennard-Jones interaction between oppositely charged sites is necessary to avoid the Coulomb singularity that would otherwise exist for these sites. In this work we choose $A_{OH} = 225.2$ kcal mol^{-1} Å^{12}, consistent with earlier extended RISM calculations.[11,24]

The solute is coupled to the solvent via Lennard-Jones and charge parameters that vary along the reaction coordinate.[1] The CH_3 moiety interacts with the solvent as a single structureless particle with total charge equal to that of the constituent atoms.[5,14,15] Otherwise, the interaction parameters of the reaction complex are as described in ref 1a for $|r_A| > 1.0$ Å. The following discussion pertains solely to the region in the neighborhood of the transition state, $|r_A| \leq 1.0$ Å, where we have examined the energy surface in detail and reparametrized the potentials. In earlier work, the solute–solvent interaction in this region was characterized only via interpolation between the transition state ($r_A = 0$) and values at $|r_A| > 1$ Å.

We consider the solute site model charge distribution first. The solute Mullikan atomic charge population analysis, obtained from the quantum chemical calculations, is the most obvious source for this parametrization. To determine whether these charges could, in fact, be used directly to provide the electrostatic parameters in the models, we have carried out a comparison of the electrostatic energies obtained by alternative routes, for several different solvent molecule–reactant complex geometries. Specifically, for a model water molecule placed in a particular relative geometry, we compare the electrostatic interaction energy computed by using (1) the quantum chemical electrostatic field evaluated from the solute wave function, (2) the field due to the

(18) Herzberg, G. *Infrared and Raman Spectra of Polyatomic Molecules*; Nostrand: New York, 1945.
(19) Ishida, K.; Morokuma, K.; Komornicki, A. *J. Chem. Phys.* **1977**, *66*, 2153.
(20) Hirata, F.; Rossky, P. J.; Pettitt, B. M. *J. Chem. Phys.* **1983**, *78*, 413, and references therein.
(21) Singer, S. J.; Chandler, D. *Mol. Phys.* **1985**, *55*, 621.
(22) Pettitt, B. M.; Rossky, P. J. *J. Chem. Phys.* **1986**, *84*, 5836.
(23) Berendsen, H. J. C.; Postma, J. P. M.; Van Gunsteren, W. F.; Hermans, J. In *Intermolecular Forces*; Pullman, B., Ed.; Reidel: Dordrecht, 1981; p 331.
(24) Pettitt, B. M.; Rossky, P. J. *J. Chem. Phys.* **1982**, *77*, 1451. See also ref 11 for corrected versions of Figures 4 and 5.

Table I. Comparison of Electrostatic Contributions to Solvent–Reactant Interaction Energies

	Mullikan charges[b]				energies[c]			
geometry[a]	q_{Cl}	$q_{Cl'}$	q_C	q_H	6-31G*[d]	Mullikan[e]	united atom[f]	ref 1[g]
1	−0.746	−0.746	−0.293	0.262	−6.24	−6.41	−6.11	−6.23
2	−0.746	−0.746	−0.293	0.262	−9.40	−10.25	−10.07	−10.44
3	−0.109		−0.536	0.215	−0.33	−1.25	−0.74	−1.49
4	−0.243	−0.975	−0.474	0.231	−13.59	−14.41	−14.56	−14.45

[a] See definition in text, section II.C. [b] Mullikan population analysis atomic charges, in units of the magnitude of the electron charge. [c] Energies in kcal/mol. [d] From quantum chemical electrostatic potentials of 6-31G* solute wave function. [e] From all-atom representation with Mullikan atomic charges. [f] From united atom representation of CH_3 with Mullikan atomic charges summed for this moiety. [g] From earlier all-atom model.[1]

Table II. Gas-phase Geometry, Energy, and Model Potential Parameters of Reactants in the Transition-State Region[a]

R_A	$r_{CCl'}$	r_{CCl}	$q_{Cl'}$	q_{Cl}	q_{CH_3}	$10^{-6}A_{Cl'O}$	$10^{-6}A_{ClO}$	$C_{Cl'O}$	C_{ClO}	E^b
0.0	2.3825	2.3825	−0.7460	−0.7460	0.4920	4.0016	4.0016	968.40	968.40	3.5693
0.01	2.3876	2.3776	−0.7498	−0.7421	0.4919	4.0042	3.9988	969.95	966.84	3.5674
0.05	2.4077	2.3577	−0.7649	−0.7263	0.4912	4.0148	3.9843	977.22	959.76	3.5223
0.10	2.4316	2.3316	−0.7828	−0.7054	0.4882	4.0261	3.9562	989.04	948.74	3.3816
0.15	2.4552	2.3052	−0.7995	−0.6839	0.4834	4.0297	3.8804	1014.2	926.99	3.1482
0.25	2.4993	2.2493	−0.8301	−0.6373	0.4675	4.0297	3.3823	1123.3	850.55	2.4112
0.36	2.5460	2.1860	−0.8596	−0.5824	0.4420	4.0297	3.2098	1153.5	832.72	1.2134
0.45	2.5850	2.1350	−0.8804	−0.5368	0.4172	4.0297	3.0994	1171.9	822.40	−0.0240
0.57	2.6389	2.0689	−0.9038	−0.4762	0.3800	4.0297	2.9756	1191.6	811.56	−1.9267
0.775	2.7472	1.9722	−0.9332	−0.3855	0.3187	4.0297	2.7992	1218.5	796.93	−5.3204
1.0	2.8976	1.8976	−0.9535	−0.3144	0.2680	4.0297	2.6919	1234.2	786.96	−8.2716

[a] Distances in Angstroms, charges in units of the magnitude of the electron charge, energies in kcal/mol. $A_{CH_3O} = 2.2368 \times 10^6$, $C_{CH_3O} = 1225.2$, and $A_{HCl} = 4 \times 10^3$, $C_{HCl} = 0$, all constant. [b] Ab initio 6-31G* energy relative to separated reactants, kcal/mol.

full set of Mullikan atomic charges, (3) the set of charges obtained from (2) by placing the sum of the C and three H charges on the carbon center (the united atom model), and (4) the result obtained by using the site charges appropriate to the earlier model[1] where the parameters were obtained by fitting to quantum chemical interaction energies.

To make this comparison, we use the TIP4P water model[25] employed in earlier work[1] so that the results obtained with that full model could be included in the comparison (4, above). The TIP4P model is a somewhat more faithful model of liquid water than the SPC model but differs only in relatively subtle ways from it. The main difference is that the negative charge associated with the oxygen atom in the SPC model is offset in TIP4P toward the hydrogens by a small distance along the HOH angle bisector. (The corresponding charge parameters that are used are correspondingly somewhat larger.)

The comparison is carried out at four representative relative geometries designed to test the interaction both at hydrogen bonding positions and at a position where interaction with the methyl group is relatively strong. These geometries (corresponding to the notation in Table I) include (1) the optimized transition state of the $Cl{-}CH_3{-}Cl$ complex, with the water molecule placed with the oxygen atom in the reactant CH_3 plane 3.6 Å from the carbon, the water C_2 axis intersecting the carbon atom (H's toward solute) and bisecting the HCH angle, and the water molecular plane perpendicular to the CH_3 plane. Geometries 2–4 correspond precisely to those given in earlier work (ref 1, Figure 4); they are (2) the transition state, as in (1) but with water at its optimal energetic position (as determined in ref 1) with respect to the transition state (at the Cl end), (3) water interacting optimally with the separated methyl chloride reactant, and (4) water interacting optimally with the ion–dipole complex of chloride with methyl chloride.

The results are shown in Table I and demonstrate that the Mullikan charges reproduce the quantum electrostatic field results quite well. Further, the united atom CH_3 model retains a completely comparable degree of accuracy. This latter observation is in contradiction to speculation in an earlier study that motivated an alternative prescription for the CH_3 charge.[5] Finally, the fact that the electrostatic energies and charges obtained via the present route agree well with the results of the earlier model from Jorgensen's laboratory shows that the Lennard-Jones A and C parameters determined there can be carried over to the present calculation, without refitting of those parameters.

There is one minor modification of the Lennard-Jones parameters that is required. In the original prescription, the chlorine–water oxygen parameters have a discontinuous derivative at the transition state, leading to the same phenomenon for the free energy surface. Since a major aim of the present work is to examine the shape of the transition-state region, this unphysical behavior is unacceptable. To repair this problem with the least quantitative effect on the free energy values, we calculate the Lennard-Jones parameters for $|r_A| \leq 1.0$ Å from a cubic spline interpolation between values given by the original function.

Specifically, for the C parameters, the spline is determined by values of the *original* function[1] at $r_{CCl'}$ values corresponding to r_A in the range from −5 to +5 Å, including only the value at $r_A = 0$ between +1 and −1 Å. For A, we use r_A values from +5 to −0.1 Å, excluding any values between −0.1 and +1.0 Å. (For $r_A \leq -0.1$ Å, A is constant, so zero slope is enforced at $r_A = -0.1$ Å.) As is true of the original function, we use the value of $r_{CCl'}$ in our computed geometries to determine the values of A and C at each point on the MEP with $|r_A| \leq 1.0$ Å. The procedure described fixes continuity with the earlier parameters for $|r_A| \geq 1.0$ Å.

The values of A_{ClO} and C_{ClO} used at the computed points on the MEP are included in Table II, along with the site charges used, obtained from the Mullikan analysis.

The final element of our model is the necessary repulsive A_{HCl} term (in analogy to the O–H term for water) for which we have used $A_{HCl} = 4 \times 10^3$ Å^{12} kcal/mol, consistent with earlier work.[11]

We note that, as in the earlier cited simulation studies, in the present study we do not address the contribution to reaction rates associated with variations in reactant complex vibrational degrees of freedom, nor do we consider in the model any direct response (polarization) of the solute charge distribution to the solvent configuration. Such potential enhancements are beyond the scope of the present study and would preclude direct comparison of the present results to those of the simulations.

III. Results

In this section, we describe the results for the gas-phase and solvated energy and free energy surfaces as well as the results for corrections to transition-state theory.

A. Gas-Phase Reaction. We begin our discussion of the results with the gas-phase potential energy surface in the region around the transition state. The numerical energetic results of our

(25) Jorgensen, W. L.; Chandrasekhar, J.; Madura, J. D.; Impey, R. W.; Klein, M. L. *J. Chem. Phys.* **1983**, *79*, 926.

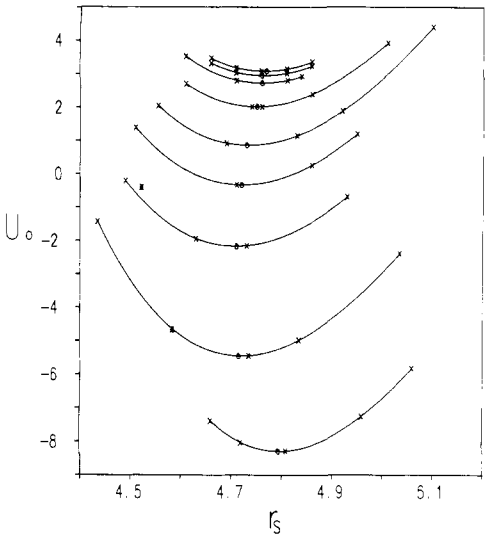

Figure 1. Gas-phase electronic energy surface for reactant configurations around the MEP in the vicinity of the transition state. Each parabola describes the energy as a function of r_S for constant r_A (see text). In order of decreasing energy at the minimum, the parabolas correspond to r_A = 0.05, 0.10, 0.15, 0.25, 0.36, 0.45, 0.57, 0.775, and 1.0 Å. Crosses and circles are the quantum chemical results from this work; circles denote points on the MEP. The two points indicated by asterisks are from ref 1, for r_A = 0.538 and r_A = 0.772, respectively, in order of decreasing energy. Energies are in kcal/mol, distances in angstroms.

calculated MEP for $|r_A| \leq 1.0$ Å are summarized in Table II. For larger values of r_A the results correspond with those published earlier.[1] The energy surface for reactant configurations around the MEP is depicted in Figure 1 as a function of symmetric stretch for selected values of asymmetric stretch, corresponding to r_A. In this work, focusing on the transition-state region, the reaction coordinate was determined by minimizing the energy with respect to the symmetric stretch coordinate for configurations of constant asymmetric stretch. This method yields the geometry of lowest energy for given r_A, which is not the same as finding the r_A for which the energy is a minimum for given r_{CCl}.[1] Representative points for this system calculated by this second procedure are included in Figure 1. As is clear from the figure, the latter procedure does not consistently correctly identify the MEP. The pitfalls of using this latter method, in which one degree of freedom is arbitrarily chosen to be held constant during geometry optimization, for construction of reaction coordinates have been discussed,[19,26] and the identification of this type of behavior is not new here. We emphasize that for regions *not* close to the transition state, the symmetric and asymmetric stretch coordinates are not particularly adapted to the description of the MEP and the approach adopted here is not of special merit.

B. Aqueous-Phase Reaction: Equilibrium Solvation Thermodynamics. The free energy surface for our model of the S_N2 reaction between Cl^- and CH_3Cl' along a reaction coordinate for collinear approach at 25 °C is shown in Figure 2, parametrized by r_A. The potential of mean force (PMF), which gives the average force acting on the reaction species at r_A, is given by

$$W(r_A) = A^{ex}(r_A) - A^{ex}(r_A=\infty) + U_0(r_A) \qquad (3)$$

$U_0(r_A)$ is the gas-phase interatomic potential energy of the reaction species at r_A, and A^{ex} is the excess free energy due to the solvent (eq 1). $U_0(r_A)$ is obtained from the gas-phase quantum mechanical energy results by subtracting from the energy of each configuration the energy of the reactants at infinite separation (see Table II).

The free energy surface is very similar to those obtained via computer simulation[1] and extended RISM[14] for other water models and for which the salient features have been discussed.[1] Briefly, hydration of the reactants flattens the ion–dipole potential minimum and substantially increases the barrier to reaction. Both

(26) Dewar, M. J. S.; Kirschner, S. *J. Am. Chem. Soc.* **1971**, *93*, 4291. Dewar, M. J. S.; et al. *Ibid.* **1971**, *93*, 4292.

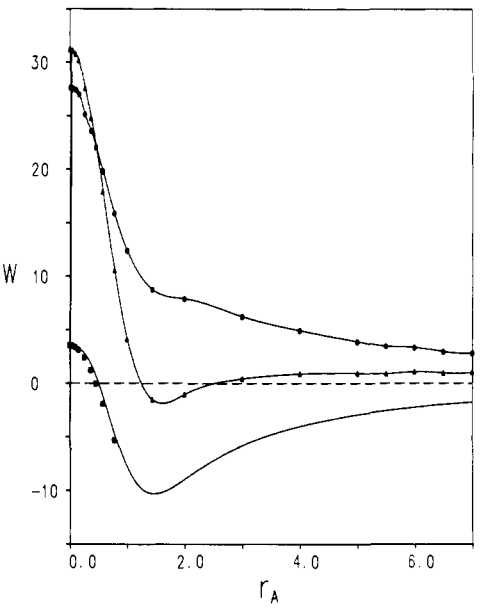

Figure 2. Potential of mean force at 25 °C for the S_N2 reaction between Cl^- and CH_3Cl as a function of asymmetric stretch r_A (see text). Triangles are $W(r_A)$; circles are $\Delta A^{ex}(r_A)$; squares are quantum chemical gas-phase potential energies from this work; the line is the gas-phase potential energy function given by eq 5 of ref 1. Units are as in Figure 1.

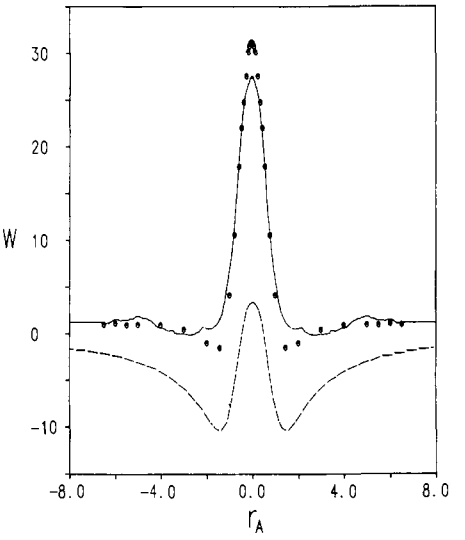

Figure 3. Comparison of present result for potential of mean force (circles), with Monte Carlo results from ref 1 (solid line); dashed line is the gas-phase energy. The simulation results have been shifted to reflect the nonzero value obtained here at 7.0 Å (see text). Units are as in Figure 1.

of these features are related to the strong solvation of the anionic nucleophile.[1] In solution, the stabilizing effect of the formation of the ion–dipole complex is offset by the work required to desolvate the anion, resulting in a surface that is relatively featureless until the onset of the barrier. Similarly, the barrier is higher in solution simply because less solvent stabilization is imparted to the diffuse charge-transition state than to the charge-localized reactants.

Comparison of the present extended RISM and Monte Carlo results from Jorgensen's laboratory is made in Figure 3. The RISM theory yields a barrier height of 31.2 kcal/mol, slightly larger than the quoted simulation and experimental results of 26.3 and 26.6 kcal/mol, respectively.[1] The integral equation calculations required approximately 500 s (Cray X-MP), a factor of more than 10^2 less time than the simulation. In the Monte Carlo calculation, the absolute value of the PMF is not determined; the PMF was set to be zero at r_A = 6.6 Å. However, the extended

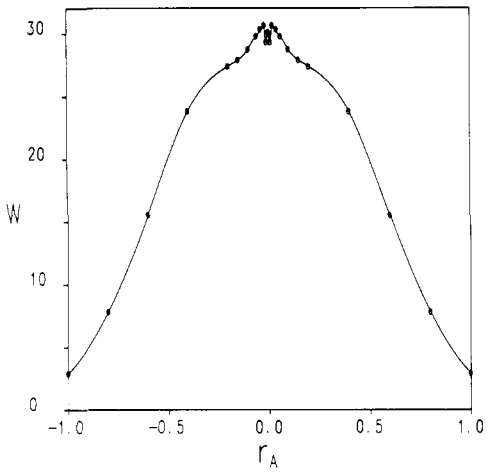

Figure 4. Integral equation result for the potential of mean force in the region immediately around the transition state for the original model used in the simulation of ref 1 (see Figure 3); 25 °C. Units are as in Figure 1.

RISM results indicate that the relative free energy of the system at r_A = 7.0 Å is still approximately 1 kcal/mol. The simulation results, as presented in Figure 3, have been adjusted accordingly.

It may be noted in Figure 3 that the PMF computed via simulation appears to have a small dip in the free energy at the transition state. Although this behavior is within the statistical noise of the simulation, if is of interest to examine this region of the free energy surface with the present approximate, but noise-free, integral equation method to establish the shape of the barrier region that would follow from the original specifitcation of the model,[1] as used in the simulations.

The result of this calculation is shown in Figure 4. As is clear from the figure, the present result clearly manifests an inverted cusp at the transition state and two inflection points on either side of this point. This behavior is consistent with the results of the simulation shown in Figure 3 and can be traced to the functional form of the solute–solvent potential and limited data used in representing the transition state region in ref 1. As is evident from Figure 2, a thorough treatment of the parametrization in this same region leads to a physically reasonable, inverted parabolic, barrier.

We note that the ability to examine such details of the free energy surface without limits on statistical accuracy or computational cost constraints represents a major advantage of the integral equation method. The same properties of the present approach permit a precise subdivision of the free energy into energetic and entropic contributions, a division that is difficult to accomplish with statistical significance via simulation.[1,27]

The energetic and entropic profiles for reaction are plotted in Figure 5. These quantities were calculated for a mean temperature T of 27.5 °C, using the method of finite differences, from the free energies computed at 25 and 30 °C, and densities corresponding (experimentally) to a fixed pressure of 1 atm according to

$$-T\Delta S = T(\partial W_S/\partial T); \quad \Delta E_S = W_S + T\Delta S \qquad (4)$$

where W_S includes only the solvation contribution to W (eq 4). The energetically dominated differential solvation of the reactants and transition state is evident from the results, in accord with expectations. Both the energetic and entropic contributions are greatest for the transition state, reflecting the relatively less favorable, and therefore less restrictive, interactions of the transition state with the surrounding solvent.

As an illustration of the differential solvation effect for this reaction, we investigate the variation of the free energy surface with solvent polarity for three fictitious, water-like solvents. For this purpose we use our modified SPC model (see above) with the sole change being that the solvent site charge q_H is equal to

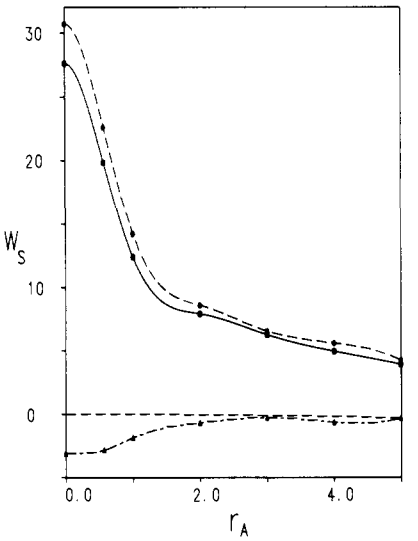

Figure 5. Thermodynamic contributions to the Helmholtz free energy of solvation W_S at 27.5 °C. W_S, solid line; ΔE_S, dashed; $-T\Delta S$, dash–dot line (see eq 4). Cubic spline curves are drawn through calculated data points as a guide to the eye. Units are as in Figure 1.

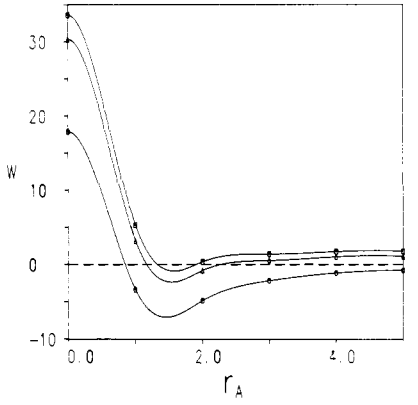

Figure 6. Variation of the reaction free energy profile with solvent polarity at 25 °C. Results shown: squares, q_H = 0.45e; triangles, q_H = 0.25e; circles, q_H = 0.10e; compared to the SPC q_H value of 0.41e. The results given are evaluated with the solute–solvent potential model of ref 1. Cubic spline curves are drawn through the calculated data points. Units are as in Figure 1.

0.10e, 0.25e, and 0.45e, respectively, for the three systems, and the model parameter for the oxygen site charge is scaled accordingly to maintain overall solvent neutrality. For comparison, the SPC model has a q_H of 0.41e.

The results are presented in Figure 6. Notice that the bimodal shape of the intrinsic gas-phase profile is increasingly manifest in the less polar solvents, with the ion–dipole minimum being enhanced, and the barrier height decreasing. The lower barrier to reaction in the slightly polar solvent reflects the lesser solvation energy of the reactants, which serves to enhance the reactivity of the nucleophile over that in the strongly polar case.

The results also show that the change in activation free energy is larger for a change in solvent polarity for the less polar model solvents compared to the more polar. This effect is seen more clearly in Figure 7, where we show the variation of the activation free energy of hydration with solvent polarity, including additional model solvents. The solvent contribution to the free energy tends to saturate for solvents of larger polarity. This type of behavior is derivable even in the context of a Born model[28] for ionic solvation if one views the localized charge reactant to diffuse charge-transition-state change as equivalent to an increase in ionic radius for a spherical ion. The nonzero intercept at zero solvent polarity

(27) Fleischman, S. H.; Brooks, C. L., III *J. Chem. Phys.* **1987**, *87*, 3029.

(28) Bockris, J. O'M.; Reddy, A. K. N. *Modern Electrochemistry*; Plenum: New York, 1970; Vol. I.

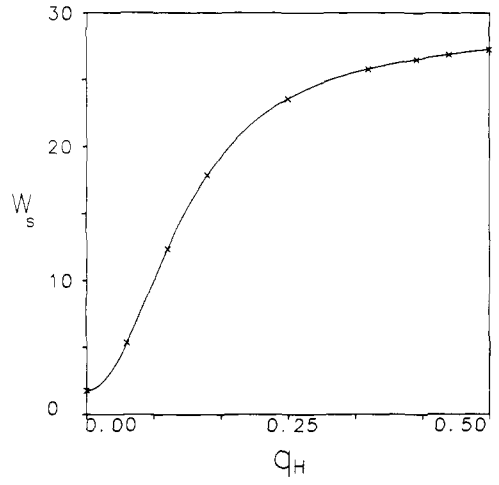

Figure 7. Variation of hydration contribution to the free energy of activation, $W_S(r_A = 0)$, with solvent polarity at 25 °C. Values calculated (×) with solute–solvent potential of ref 1; the curve is a cubic spline fit. Energies in kcal/mol, charges in units of e.

($q_H = 0$), however, is indicative of a small (~1.5 kcal/mol) barrier arising from packing forces alone, due to a slightly larger volume for the transition-state complex compared to the reactants.[7]

C. Corrections to Transition-State Theory Rate Constants. It is widely appreciated that transition-state theory rate constants represent an approximation to the correct result due to the exclusion of multiple crossings of the transition state in the formulation of the theory. The latter arise, in general, from the coupling of the reactant dynamics with fluctuations in the solvent. The role of this coupling in the dynamics of barrier crossing has been analyzed in some detail by Hynes and co-workers.[8] In this analysis, the emphasis has been placed on the direct participation of the solvent in the reaction coordinate. At one extreme, the reactants respond instantaneously to the solvent motion (e.g., in the case of electron transfer), so that the solvent motion governs the reaction progress. In the other extreme, it is the solvent that equilibrates to the reactant motion. The latter case is also that implicit in the use of a reactant free energy surface in solution to describe the course of reaction, as was done above.

This latter case has been referred to as that of equilibrium solvation,[8] while deviations are termed nonequilibrium solvation. In the generalized theory,[8] the degree of dynamical coupling is introduced in terms of a generalized frictional force acting on the reactants which accounts for the deviations from equilibrium solvation.

In a recent large-scale simulation study[5] of a model S_N2 reaction with a molecular model comparable to that used here, it was found that the solvent dynamical behavior during crossing events was the antithesis of the adiabatic picture implicit in the use of solvation free energies. There it was found that to good accuracy, the outcome of a crossing event was determined by the instantaneous configuration of the solvent at the time of crossing. This "frozen" or nonadiabatic solvent limit corresponds to a dynamical decoupling of the solvent and reactant with the reactant dynamics being much faster. Hence, in essence, the reaction rate is determined by an average over the instantaneous solvent configurations occurring at the reactant transition state of the reaction probability for each configuration. Such information is completely contained in the distribution of fluctuations *at equilibrium*. Correspondingly, it is reasonable that one may evaluate the required quantities to correct the transition-state theory in this case from a purely equilibrium calculation. In this section, we show how this can be done within the integral equation framework for the present, charge-transfer, reaction.

The quantity of interest is κ, the ratio of the rate constant k to the transition-state theory result k^{TST}. The nonadiabatic solvation theory yields the following expression for κ in the frozen-solvent limit:[8]

$$\kappa = [1 - \beta(\langle(\delta F_S)^2\rangle/\mu\omega_{b,eq}{}^2]^{1/2} \tag{5}$$

δF_S is the fluctuation of the solvent force along the reaction coordinate, μ is the appropriate mass for motion along the reaction coordinate,[18] and $\omega_{b,eq}$ is obtained from the magnitude of the curvature of the free energy barrier at the transition state. Here, we preserve the notation of ref 8c where possible.

To evaluate this expression, we need to relate $\langle(\delta F_S)^2\rangle$ to a result obtainable from the integral equation calculation. The solvent contribution to the reaction free energy is, within an additive constant

$$A^{ex}(r) = -k_B T \ln (Z_S(\mathbf{r})) + \text{constant} \tag{6}$$

where

$$Z_S(\mathbf{r}) = \int ds\, e^{-\beta U(\mathbf{r};\mathbf{s})} \tag{7}$$

Here $\mathbf{r}$ is the set of reactant solute (u) coordinates, $\mathbf{s}$ is the complete set of solvent (v) coordinates, and $U(\mathbf{r};\mathbf{s})$ is the potential energy function given by

$$U(\mathbf{r};\mathbf{s}) = [U_{uv}(\mathbf{r};\mathbf{s}) + U_{vv}(\mathbf{s})] \tag{8}$$

Note that in this calculation U_{uv} has a parametric as well as a geometric dependence on $\mathbf{r}$ because the solute–solvent Coulombic and Lennard-Jones terms are themselves functions of $\mathbf{r}$.

Differentiating $A^{ex}(\mathbf{r})$ with respect to $r_A(\mathbf{r})$ to second order, we obtain

$$\left(\frac{d^2A^{ex}}{dr_A{}^2}\right) = \left\langle\frac{d^2U_{uv}}{dr_A{}^2}\right\rangle_S - \beta\left\langle\left(\frac{dU_{uv}}{dr_A}\right)^2\right\rangle_S + \beta\left\langle\frac{dU_{uv}}{dr_A}\right\rangle_S^2 \tag{9}$$

where $\langle\ \rangle_S$ indicates an average over the solvent coordinates for fixed r. Now, any force on the reaction-complex at $r_A = 0$ is due to the solvent and derives from A^{ex}, since the gas-phase potential has zero slope at the saddlepoint. Thus we can identify the solvent bias force as $-F_S = (dU_{uv}/dr_A)|_{r_A=0}$ and recast eq 9 in terms of F_S:

$$\left(\frac{d^2A^{ex}}{dr_A{}^2}\right)\Bigg|_{r_A=0} = \left\langle\frac{d^2U_{uv}}{dr_A{}^2}\right\rangle_S\Bigg|_{r_A=0} - \beta[\langle(F_S)^2\rangle_S - \langle F_S\rangle_S{}^2] \tag{10}$$

The fluctuation in F_S can therefore be evaluated from the response-function-like expression

$$-\beta\langle(\delta F_S)^2\rangle = (d^2A^{ex}/dr_A{}^2)_{r_A=0} - \langle d^2U_{uv}/dr_A{}^2\rangle_{S,r_A=0} \tag{11}$$

The average of the last term in this expression is over the solvent ensemble characterizing the transition state.

To use this result in the calculation of κ, we denote, as force constants

$$(d^2A^{ex}/dr_A{}^2)|_{r_A=0} = -k_{eq} \tag{12}$$

$$d^2(A^{ex} + U_0)/dr_A{}^2|_{r_A=0} = -(k_{eq} + k_b) \tag{13}$$

$$\mu\omega_{b,eq}{}^2 = k_{eq} + k_b \tag{14}$$

Recognizing that the averaged quantity $\langle F_S\rangle^2 = 0$, we obtain

$$\beta\langle(\delta F_S)^2\rangle = \beta\langle F_S{}^2\rangle = k_{eq} + \langle d^2U_{uv}/dr_A{}^2\rangle_{S,r_A=0} \tag{15}$$

from eq 11. κ may thus be expressed as

$$\kappa = \left(1 - \frac{k_{eq} + \langle d^2U_{uv}/dr_A{}^2\rangle_{r_A=0}}{k_{eq} + k_b}\right)^{1/2} \tag{16}$$

It is clear from eq 15 and 16 that neglecting solvent force fluctuations yields $\kappa = 1$.

Evaluation of eq 16 for κ requires calculation of the quantity

$$\langle d^2U_{uv}/dr_A{}^2\rangle_{S,r_A=0}$$

Strictly read, this implies a full differentiation of $U_{uv}(\mathbf{r};\mathbf{s})$ with respect to $r_A(\mathbf{r})$. That is, U_{uv} depends both explicitly on the reactant coordinates and implicitly on them through the parametric dependence of the Lennard-Jones and charge coupling constants (see Table II). However, this term can be calculated for this

charge-transfer reaction in an approximate, albeit more straightforward, fashion.

The solvent-induced deviations from the TST rate have been shown to track the relative rate of charge transfer;[5] i.e., the solvent modification to the barrier is electrostatic in nature. These deviations are not strongly influenced by the relatively small geometrical changes of the solute but are strongly dependent on the rapidly shifting solute charge in the transition-state region. The latter occurs with quite small solute geometry changes. Therefore, we can obtain a good estimate of κ if we neglect the explicit dependence of U_{uv} on solute geometry changes but retain the parametric dependence of the potential. The use of this approach has obvious advantages in the present context, since the spatial solute–solvent distribution functions evaluated for a solute with the transition-state geometry are readily accessible. To use the present results, we then simply evaluate the derivative appearing in the last term in eq 15 via the *parametric* dependence of the coupling constants appearing in U_{uv} on r_A and then evaluate the average over the solvent distribution characterizing the transition state. This last step is completely analogous to the evaluation of the average potential energy and can be done by using the solute–solvent site–site correlation functions evaluated from the integral equation for the transition-state geometry ($r_A = 0$).

When applied to our system (μ = 18.214 amu; see ref 18), we find the values $\omega_b = (k_b/\mu)^{1/2}$ = 376.1 cm^{-1}, $\omega_{b,eq}$ = 542.9 cm^{-1}, and

$$(d^2U_{uv}/dr_A^2)_{S,r_A=0} = 10.06 \text{ kcal/(mol Å}^2)$$

Equation 16 then predicts a correction factor κ = 0.59, in reasonable accord with the value derived from the lengthy simulation studies[5] of 0.55.

The very close comparison should be viewed as in part fortuitous since the models used are somewhat different. Our barrier is apparently somewhat broader, and our solvent somewhat more polar, so that κ might be expected to be somewhat smaller for our system than for that simulated. At the same time, our neglect of explicit geometric dependence should lead to systematic overestimation of κ; the simulated result with no charge transfer yields κ = 0.9, while we would obtain essentially κ = 1. Nevertheless, the general agreement (both values roughly one-half) indicates that the approach is a useful and efficient one for processes dominated by the charge-transfer aspect.

IV. Conclusions

We have carried out a detailed study of the gas-phase energy and solvated, free energy surfaces for the reaction of chloride with methyl chloride in water, focusing on behavior in the transition-state region. By employing the extended RISM integral equation to treat the solvation, we have examined the free energy surface at a level of detail that is not easily accessible via simulation with its associated statistical error. Correspondingly, the energy and entropy components are readily separable here. The variation of behavior with solvent polarity has also been efficiently examined, and the tendency for saturation behavior in the activation free energy for polarities as high as that of water has been demonstrated. Using this surface and the nonadiabatic solvation theory of Hynes and co-workers, we have shown that for the limiting case of fast reaction and rapid charge transfer, the corrections to transition-state theory due to solvent fluctuations are readily calculable from the integral equation results.

The present calculations have demonstrated the importance of properly describing the variation of the interatomic potentials in the transition-state region if a physically meaningful free energy surface in this region is desired.

The integral equation method provides a valuable complement to the methods of computer simulation, providing rapid access to qualitatively reliable descriptions of reaction free energy surfaces. Application of these methods to a wider range of reactions and solvents appears very worthwhile.

Acknowledgment. Support of this work by a grant from the National Institute of General Medical Sciences is gratefully acknowledged, as is computational support from the University of Texas System Center for High Performance Computing. P.J.R. is the recipient of an NSF Presidential Young Investigator Award and a Camille and Henry Dreyfus Foundation Teacher–Scholar Award.

Registry No. CH_3Cl, 74-87-3; Cl, 16887-00-6.

Reassignment of the Structure of $Si(CO)_2$ Based on Theoretically Predicted IR Spectra

Roger S. Grev* and Henry F. Schaefer, III

Contribution CCQC No. 46 from the Center for Computational Quantum Chemistry, School of Chemical Sciences, University of Georgia, Athens, Georgia 30602. *Received January 3, 1989*

Abstract: Self-consistent-field methods show that the lowest energy structure of $Si(CO)_2$ is a strongly bent C_{2v} symmetry structure more akin to that of a transition-metal carbonyl than to its isovalent quasi-linear first-row analogue carbon suboxide. Configuration interaction predictions of isotopic shifts in C–O stretching vibrational frequencies for this isomer agree with those previously observed experimentally, as do the differences in C–O frequencies between the mono- and dicarbonyl. Thus, we suggest a reassignment of the observed spectra from that of the previously assumed $D_{\infty h}$ structure to the C_{2v} symmetry $^1A_1$ state found here.

Hypothesis

In a pioneering study on the reaction of silicon atoms with typical main-group ligands, Lembke, Ferrante, and Weltner (LFW) found[1] that silicon could add either one or two carbon monoxide molecules to form SiCO and $Si(CO)_2$, but only one of the isoelectronic nitrogen molecules would add, forming SiN_2. This was in perfect agreement with reactions of carbon atoms and CO and N_2 ligands where, once again, no compound of the form N_2CN_2 was in evidence, but CCO, $C(CO)_2$, and CNN were easily formed.

Confirmation of the formation of the dicarbonyl, $Si(CO)_2$, was provided by the appearance of the (seemingly) proper number of infrared C–O stretching vibrational frequencies after annealing

(1) Lembke, R. R.; Ferrante, R. F.; Weltner, W., Jr. *J. Am. Chem. Soc.* **1977**, *99*, 416.

0002-7863/89/1511-5687$01.50/0